Electronic Supplementary Material (ESI) for Physical Chemistry Chemical Physics.

Electronic Supplementary Information

Tailoring the Surface-oxygen Defects of Tin Dioxide Support toward Enhanced Electrocatalytic Performance of Platinum Nanoparticles

Maidhily Manikandan,[†,‡] Toyokazu Tanabe,[†,§,] Gubbala V. Ramesh,[†] Rajesh Kodiyath,[†] Shigenori Ueda,[§§] Yoshiki Sakuma,[†] Yusaku Homma,[ǁ] Arivuoli Dakshanamoorthy [‡], Katsuhiko Ariga [§§§] and Hideki Abe[†,*]*

[†] National Institute for Materials Science, 1-1 Namiki, Tsukuba, Ibaraki 305-0044, Japan.

[‡] Crystal Growth Centre, Anna University, Chennai, Tamil Nadu 600-025, India.

[§] Kanagawa University, 3-27 Rokkakubashi, Yokohama, Kanagawa 221-8686, Japan.

[§§] Synchrotron X-ray Station at SPring-8, National Institute for Materials Science, 1-1-1 Kouto, Sayo, Hyogo 679-5148, Japan.

[§§§] International Center for Material Nanoarchitectonics, National Institute for Materials Science, 1-1 Namiki, Tsukuba, Ibaraki 305-0044, Japan.

[ǁ] International Center for Young Scientists, National Institute for Materials Science, 1-2-1 Sengen, Tsukuba, Ibaraki 305-0047, Japan.

Contents

1. Materials

Tin (II) chloride dihydrate ($SnCl_2.2H_2O$, 99.995 %, trace metal basis, Sigma Aldrich), sodium citrate dihydrate ($Na_3C_6H_5O_7.2H_2O$, ≥ 99 %, Sigma Aldrich), sodium hydroxide (NaOH, ≥ 99.99 %, Sigma Aldrich), hydrogen peroxide (H_2O_2, 30 %, Wako), chloroplatinic acid hexahydrate ($H_2PtCl_6.6H_2O$, ACS reagent ≥ 37 % Pt basis Sigma Aldrich,) and sodium borohydride ($NaBH_4$, 0.1 M, ≥ 99.99%, Aldrich) were used as received.

2. Methods

2.1 Powder X-ray diffractometry (*p*XRD)

Powder X-ray diffractometry (*p*XRD) was performed using CuK_α radiation (Panalytical X'Pert PRO; λ = 0.1548 nm) with an increment of 0.02 degrees in a range of diffraction angles from 20 to 80 degrees. An obliquely finished Si crystal (non-reflection Si plate) was used as a sample holder to minimize the background.

2.2 Hard X-ray photoemission spectroscopy (HAXPES)

Hard X-ray photoemission spectroscopy (HAXPES) was performed using X-rays with photon energy of 5.95 keV at the undulator beamline BL15XU of SPring-8, Japan. Sample powder was first dispersed in tetrahydrofuran (THF) and dropped onto a carbon substrate. The sample was thoroughly dried in air and transferred into an ultra-high-vacuum (UHV) chamber attached to a high-resolution electron spectrometer (VG Scienta R4000). Total energy resolution was set to 240 meV. The binding energy of photoelectrons was referred to the Fermi energy of an Au film that was electrically contacted to the sample. The measurements were performed at room temperature.

2.3 Scanning electron microscopy (SEM)

A scanning electron microscope (Hitachi S-8000, accelerating voltage = 5.0 kV) was used for the morphological analysis of synthesized catalysts.

2.4 Transmission electron microscopy (TEM)

Transmission electron microscopy (TEM) images were obtained with a JEOL 2100-F microscope with an operating voltage of 200 kV. The composition of the SnO_2 NFs was analyzed with an energy-dispersion spectroscopy (EDS, Oxford link system) analyzer, which was attached to the TEM. The sample for TEM was prepared by dropping a methanol suspension of the sample powder onto a copper micro grid. The sample was thoroughly dried in vacuum prior to observation.

2.5 X-ray fluorescence spectroscopy (XRF)

XRF spectra were obtained with a micro XRF analyzer, Orbis I (EDAX). Samples were dispersed in isopropanol, dropped onto carbon substrates and thoroughly dried in air.

2.6 Scanning probe microscopy (SPM)

A scanning probe microscope (JSPM-5200, JEOL), equipped with a tip material of monolithic Silicon (Electrical conductive coating of 5.0 nm chromium and 25 nm Platinum on the both sides of cantilever, 3.0 Nm^{-1} force constant) was used to visualize all the KFM/AFM images. All images were collected in non-contact mode at a scan rate of 15-75 kHz.

2.7 Photoluminescence spectroscopy (PL)

PL spectra were measured at 10 K and 300 K by using a 32 cm-length monochromator (Jobin Yvon HR320) equipped with a liquid-nitrogen-cooled Si-CCD detector. The samples were placed in an optical cryostat and excited with a 325 nm He-Cd laser source of 1.4 mW output power.

2.8 Electrochemical measurements

A glassy carbon (GC) electrode (5 mm in diameter, PINE) was polished prior to use with Gamma Micropolish Alumina (Baikalsox, Type 0.05 μm CR). The GC electrode was rinsed with Milli-Q water and finally dried in air. An aliquot of 1.8 mg of the sample powder was suspended in a mixture of 1745 μl of milliQ water, 440 μl of isopropyl alcohol, and 18 μl of a 5.0 % w/w lower aliphatic alcohols-water solution of Nafion (EW: 1100, Aldrich). After sonication for 60 min, the suspension (28 $\mu g_{Pt}\ cm^{-2}$ present on the electrode surface) was dropped onto the GC electrode and dried at 60 ^oC in air. Cyclic voltammetric (CV) measurements were performed

using a computer-controlled electrochemical system (HSV-100, Hokuto Denko) in a three-electrode, one-compartment electrochemical cell (main compartment volume = 100 ml, PINE Co.). A Pt wire and an Ag/AgCl electrode (4.0 M KCl, PINE Co.) were used as the counter electrode and the reference electrode, respectively. All the voltammograms were acquired at room temperature at a potential sweep rate of 20 mVs^{-1}. The electrochemical surface area (ECSA) of the sample was determined by measuring the columbic charge for hydrogen under potential adsorption/desorption between -0.16 and +0.20 V, assuming 210 $\mu C\ cm^{-2}$ for a monolayer of adsorbed hydrogen on the platinum surface.

Stability of the Pt/SnO_2 NFs, Pt/SnO_2 NPs and Pt/C (20 wt%; E-TEK) was examined by repeatedly cycling the electrode between +0.6 and +1.2 V at a sweep rate of 50 mVs^{-1} in 0.5 M aqueous solution of H_2SO_4. Electro-oxidation of ethanol (Chameleon reagent) was carried out in aqueous solution of 1.0 M ethanol+0.5 M H_2SO_4, where the solution was de-aerated with pure Ar gas for 30 min in prior to the measurements. Before performing the electro-oxidation of ethanol, background currents were measured in de-aerated 0.5 M aqueous solution of H_2SO_4. CO stripping experiments were conducted at room temperature in 0.5 M aqueous solution of H_2SO_4. The solution was first bubbled with pure CO gas (99.9999 %) and subsequently with pure Ar gas while holding the electrode potential at 0.0 V. Two consecutive cyclic voltammogram curves were recorded at 20 $mV\ s^{-1}$ in a potential range between -0.18 to +1.0 V.

3. Supporting Figures

3.1. XRF

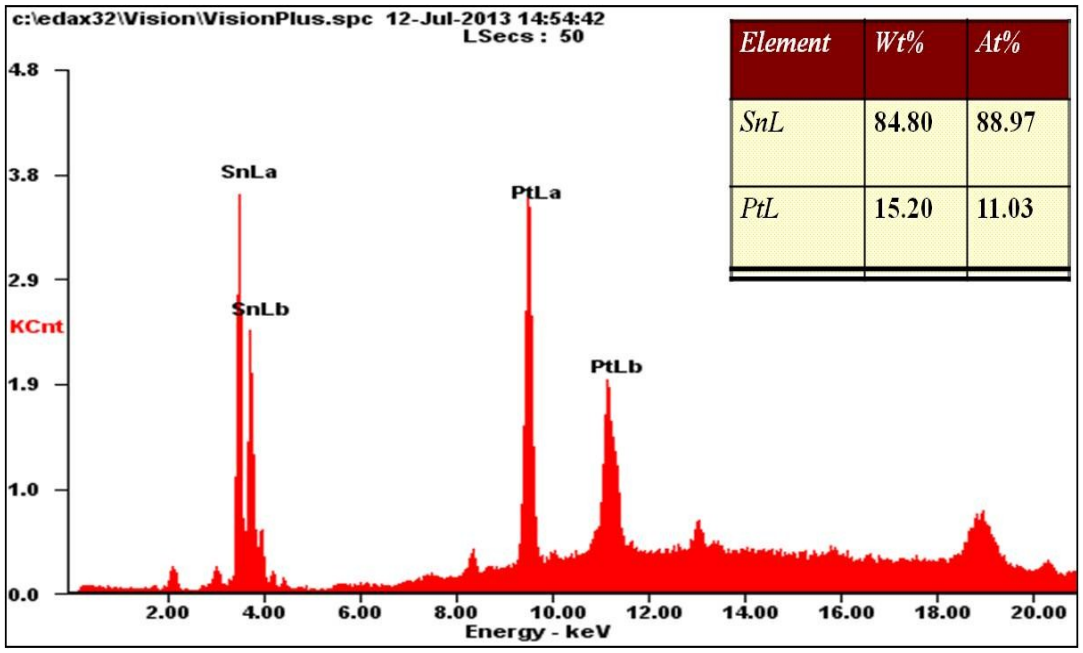

Element	Wt%	At%
SnL	84.80	88.97
PtL	15.20	11.03

S1. X-ray fluorescence analysis on the Pt/SnO_2 NFs. The weight percentage is provided as an average of the values obtained at two different points.

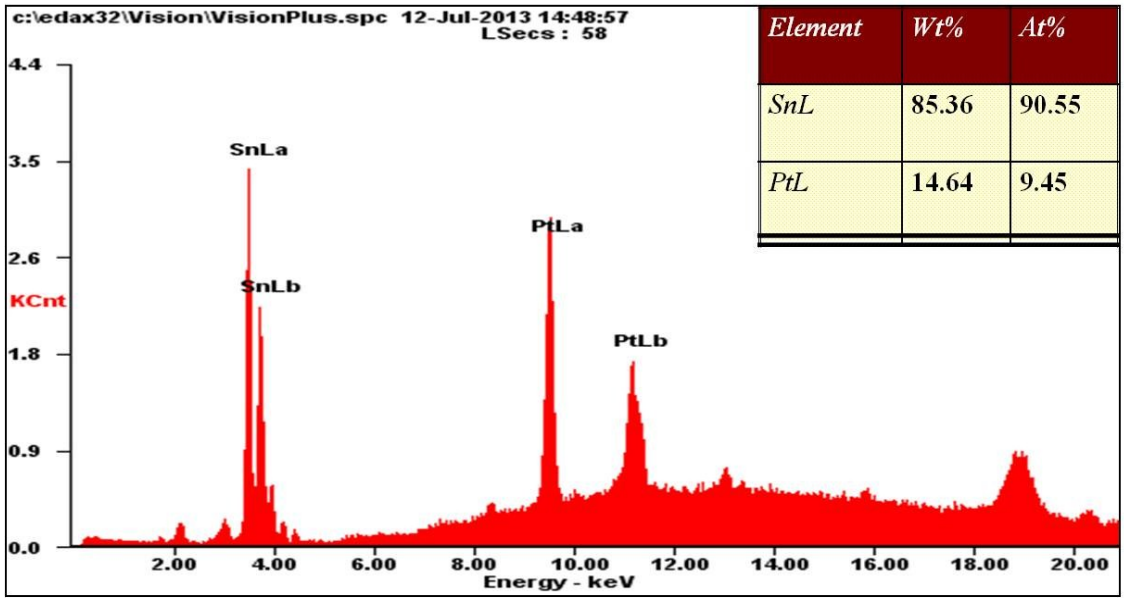

Element	Wt%	At%
SnL	85.36	90.55
PtL	14.64	9.45

S2. X-ray fluorescence analysis on the Pt/SnO_2 NPs. The weight percentage is provided as an average of the values obtained at two different points.

3.2. HAXPES

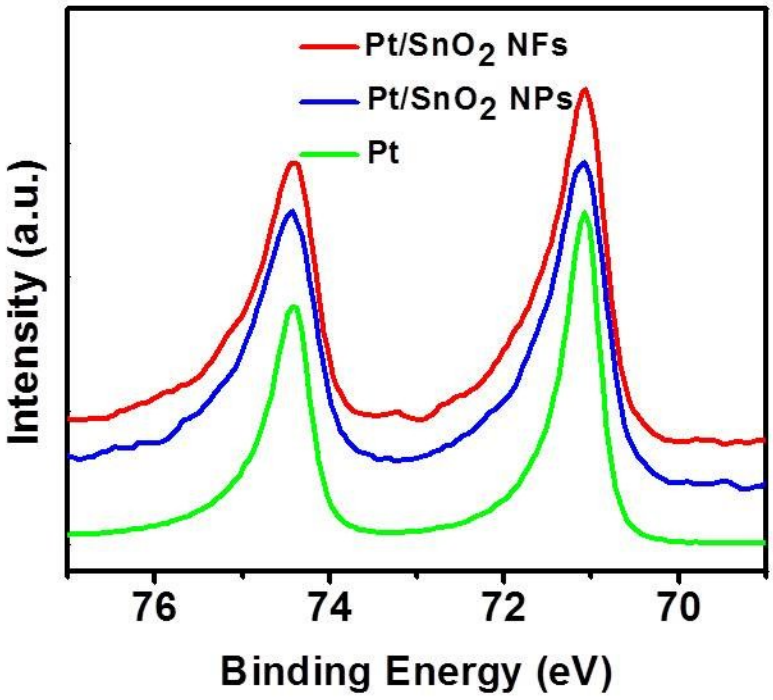

S3. HAXPES spectra in the Pt 4*f* region for the Pt/SnO_2 NFs, Pt/SnO_2 NPs and Pt standard. Note that the Pt 4*f* spectra for the Pt/SnO_2 materials are different from that for a control sample, Pt nanoparticles. This difference is attributed to $Pt^{+\delta}$ atoms at the Pt/SnO_2 interface. On the other hand, the HAXPES spectra in the Sn-core region are virtually the same regardless of the materials (Figure 1E). The Pt NPs are immobilized on the support surface mostly through $Pt^{+\delta}$-oxygen bonds, resulting in the enhanced O1*s* peak at binding energy = 533.0 eV for the Pt/SnO_2 NFs (Figure 1F).

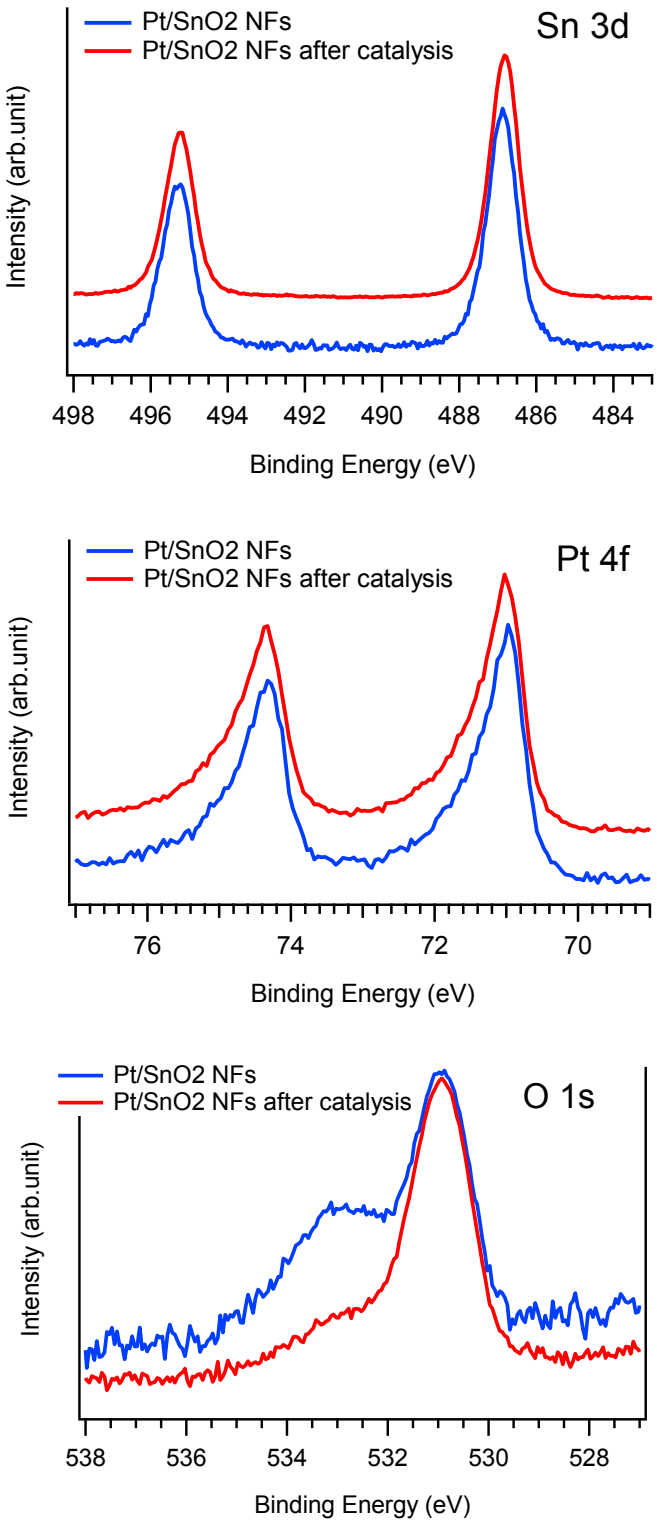

S4. HAXPES spectra for the Pt/SnO_2 NFs before and after the 10000-times repeated potential cycles.

3.3. TEM/SEM

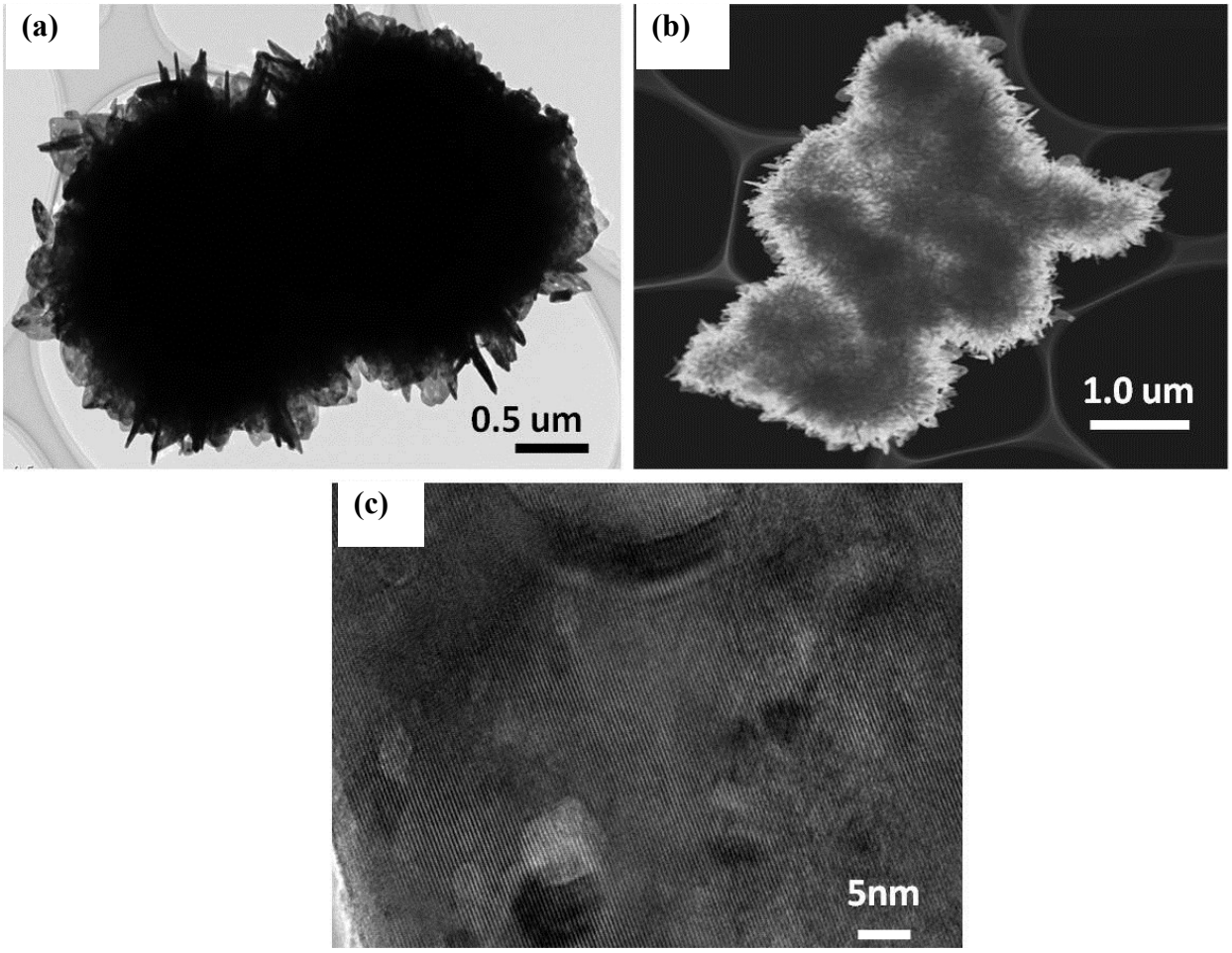

S5. (a) TEM-, (b) STEM- and (c) HRTEM images of the SnO_2 NFs.

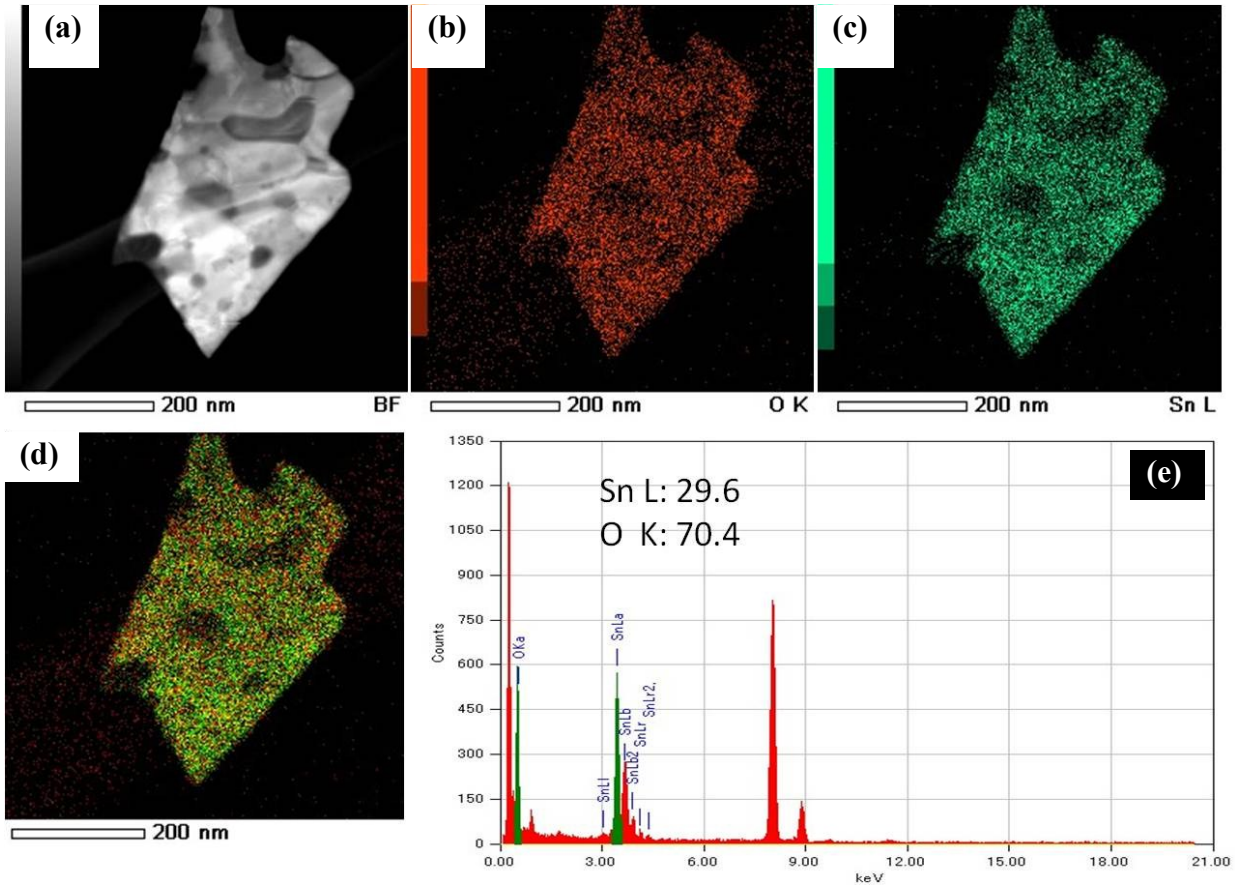

S6. (a) Annular-dark field image, (b-c) elemental-mapping images, (d) composite image and (e) elemental-analysis spectrum for the SnO_2 NFs.

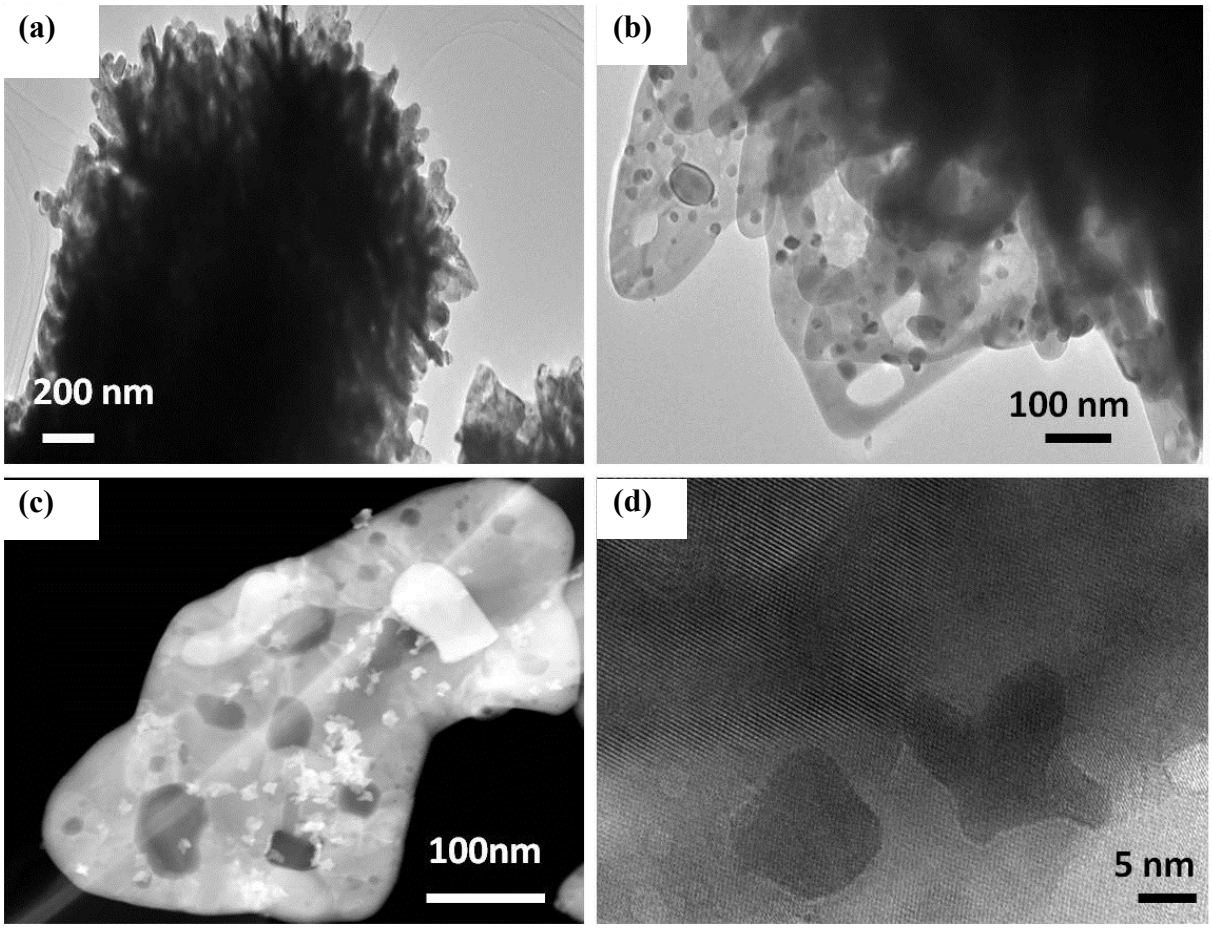

S7. (a,b) HRTEM images of the Pt/SnO_2 NFs at low magnification. (c) Annular-dark field image at low magnification and (d) at high magnification of the Pt/SnO_2 NFs.

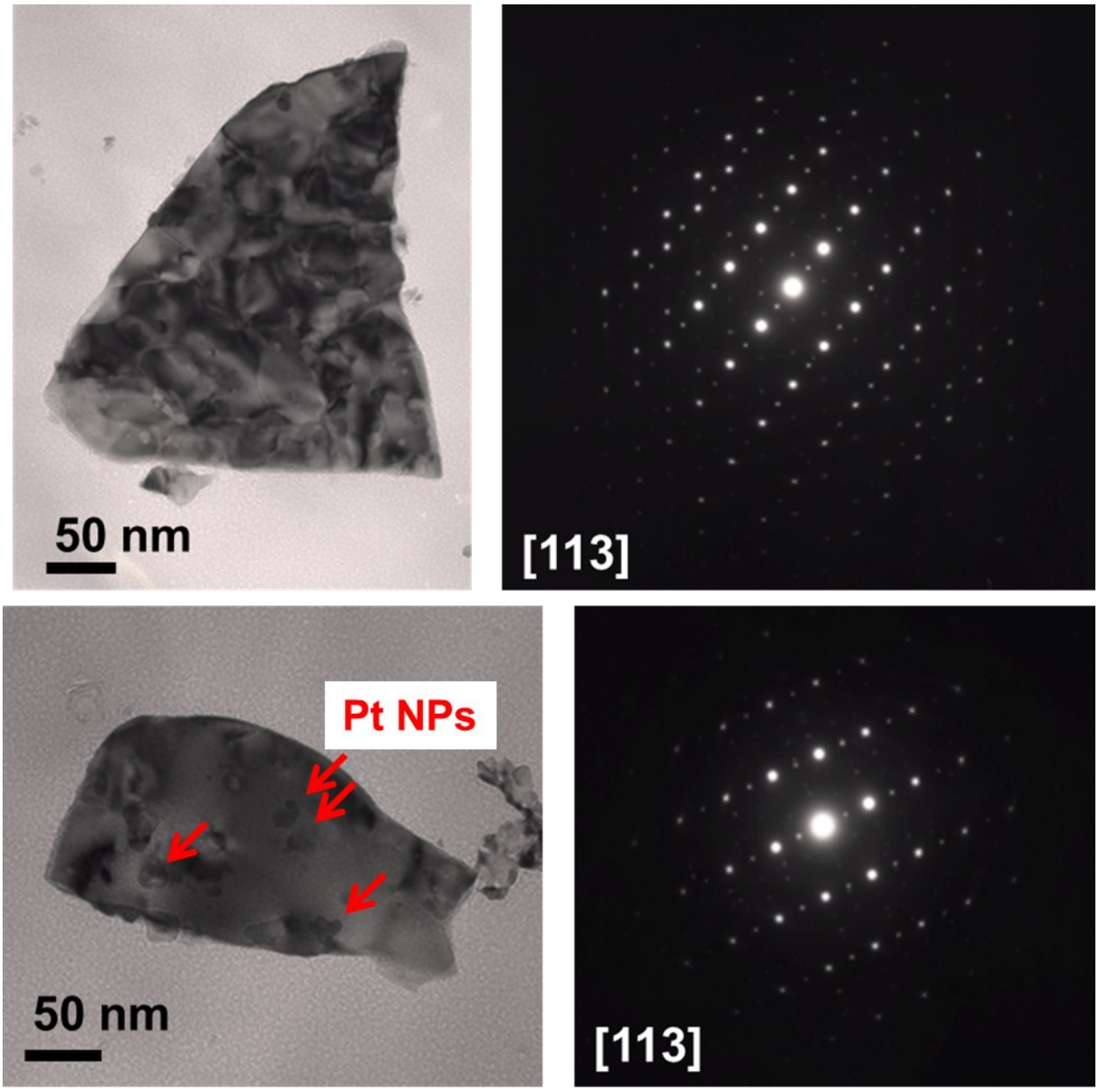

S8. TEM images and SAED patterns for the Pt/SnO_2 NFs after repeated catalysis.

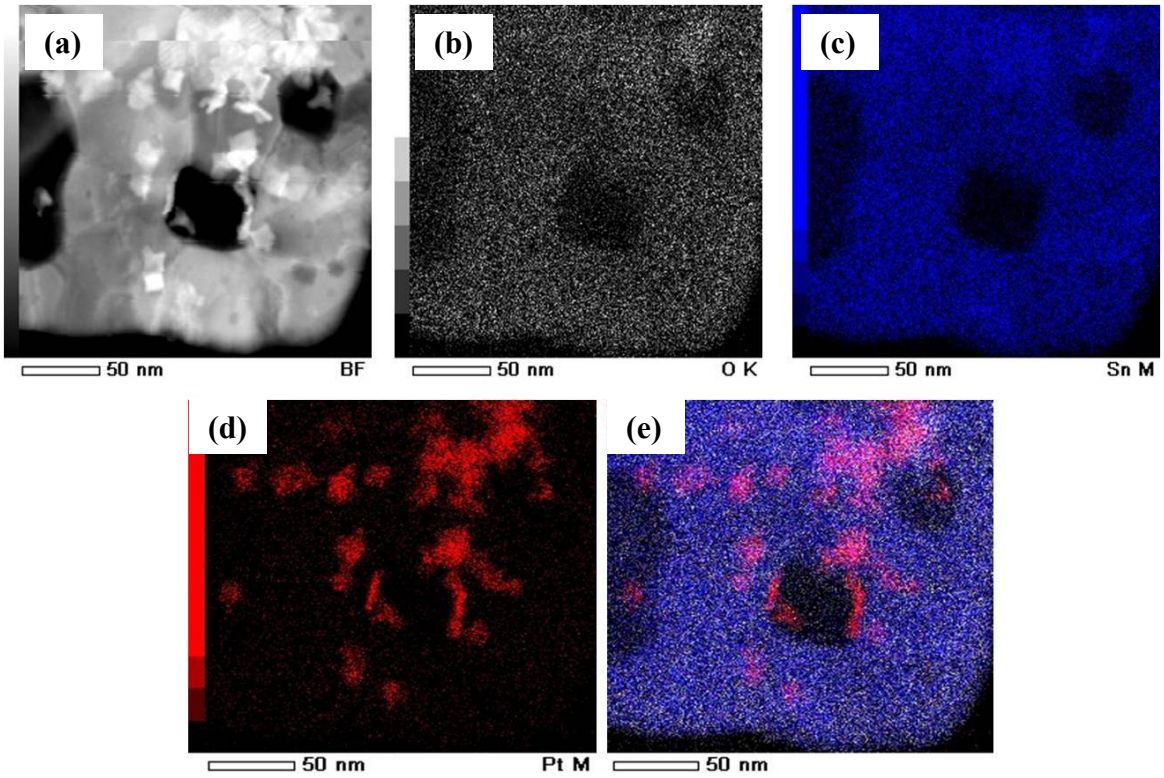

S9. (a) Annular-dark field image of the Pt/SnO_2 NFs and the corresponding elemental mapping of (b) O, (c) Sn, (d) Pt and (e) composite image.

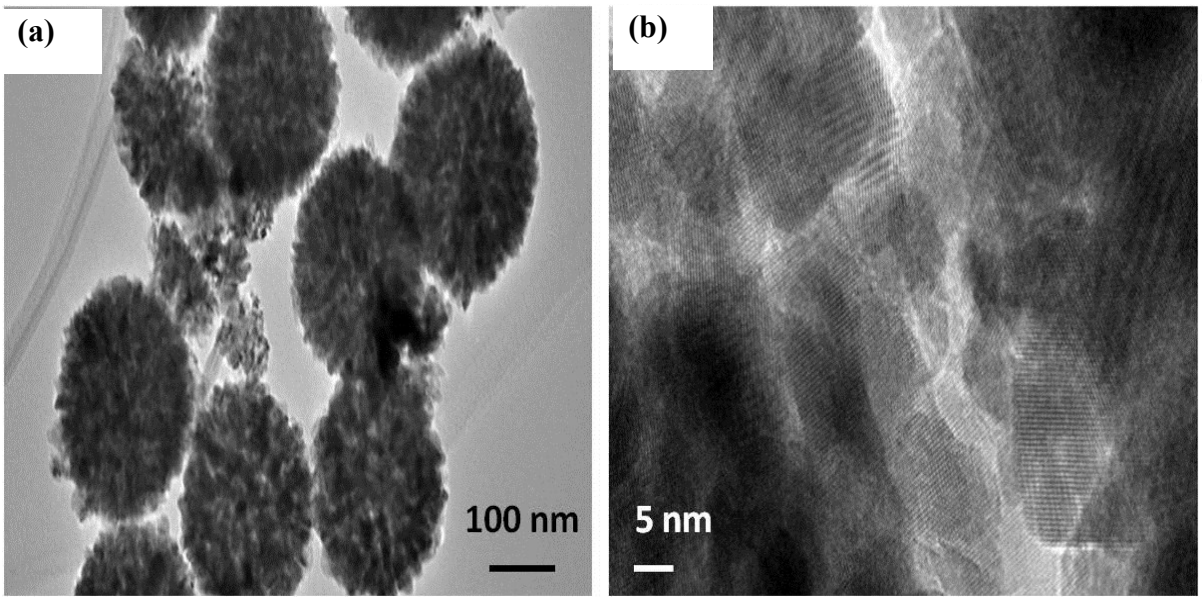

S10. (a) Low- and (b) high magnification HRTEM images of the Pt/SnO_2 NPs.

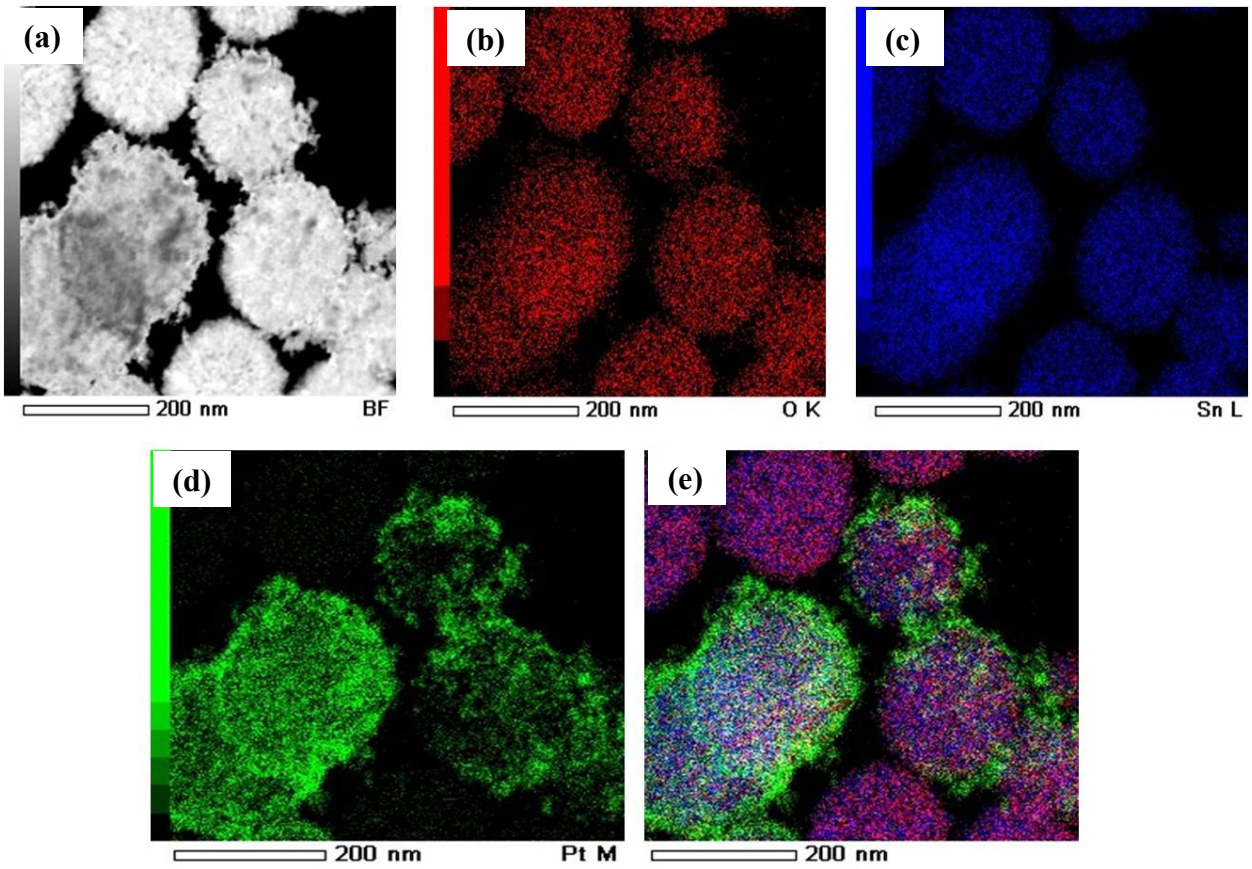

S11. (a) Annular-dark field image of the Pt/SnO_2 NPs and the corresponding elemental mapping of (b) O, (c) Sn, (d) Pt and (e) composite image.

3.4. Raman spectra

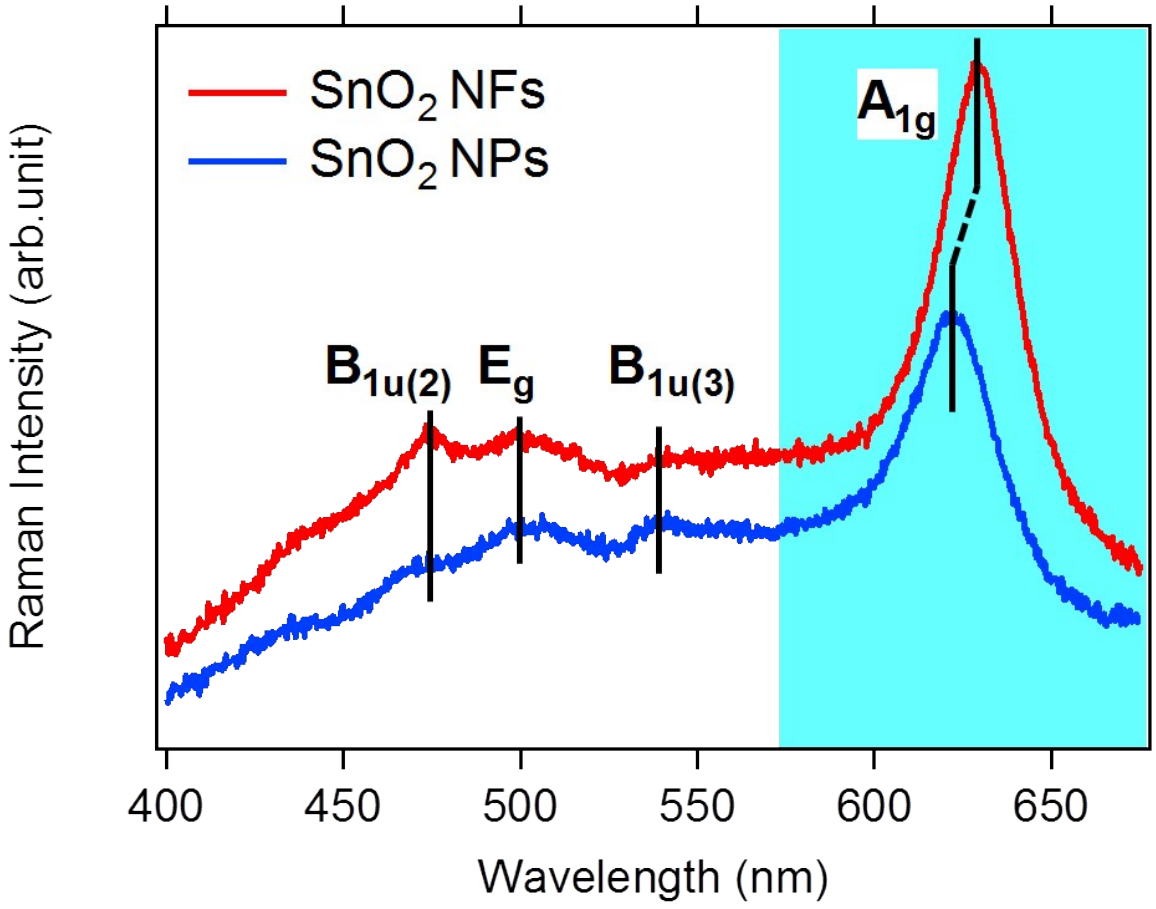

S12. Raman spectra for the SnO_2 NFs and SnO_2 NPs. Measurement temperature: 300 K. The A1g peaks at 430 nm and 420 nm for the SnO_2 NFs and SnO_2 NPs are attributed to oxygen defects in bridge-site- and sub-bridge-site configurations, respectively (L. Z. Liu , T. H. Li , X. L. Wu , J. C. Shen and P. K. Chu, *J. Raman Spectroscopy* ,2011, **43**, 1423-1426.).

3.5. Electrochemical profiles

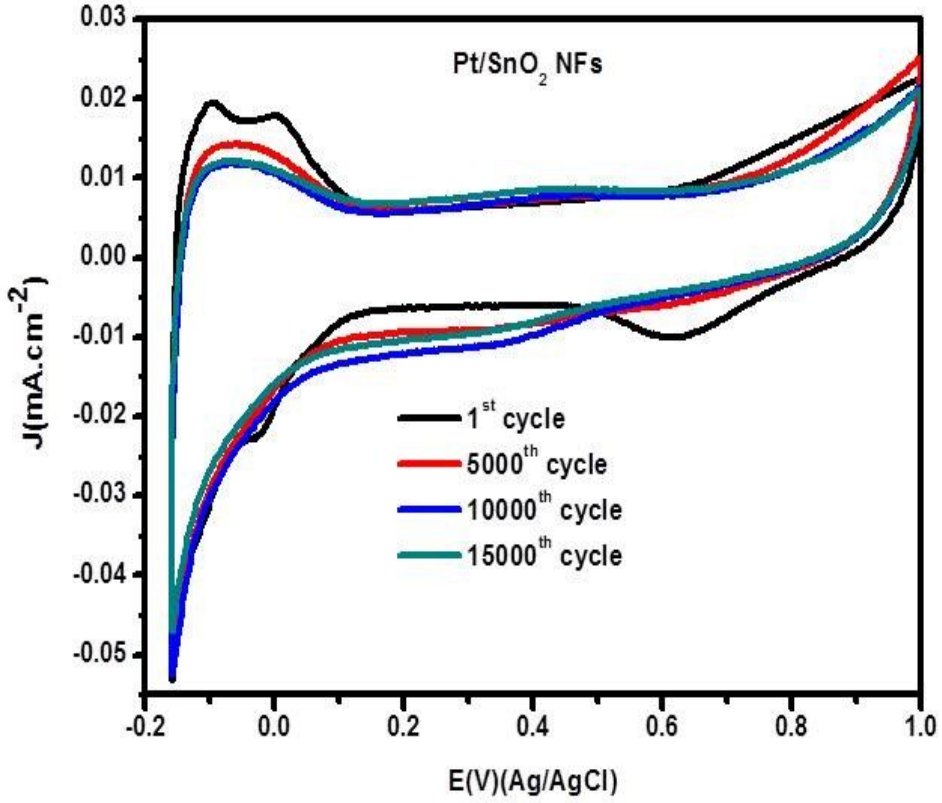

S13. Cyclic voltammograms of the Pt/SnO_2 NFs, recorded in between the stability test conducted in 0.5 M H_2SO_4 between +0.6 and +1.2V at a scan rate of 50 mVs^{-1}. The given curves were measured at a scan rate of 20 mVs^{-1}.

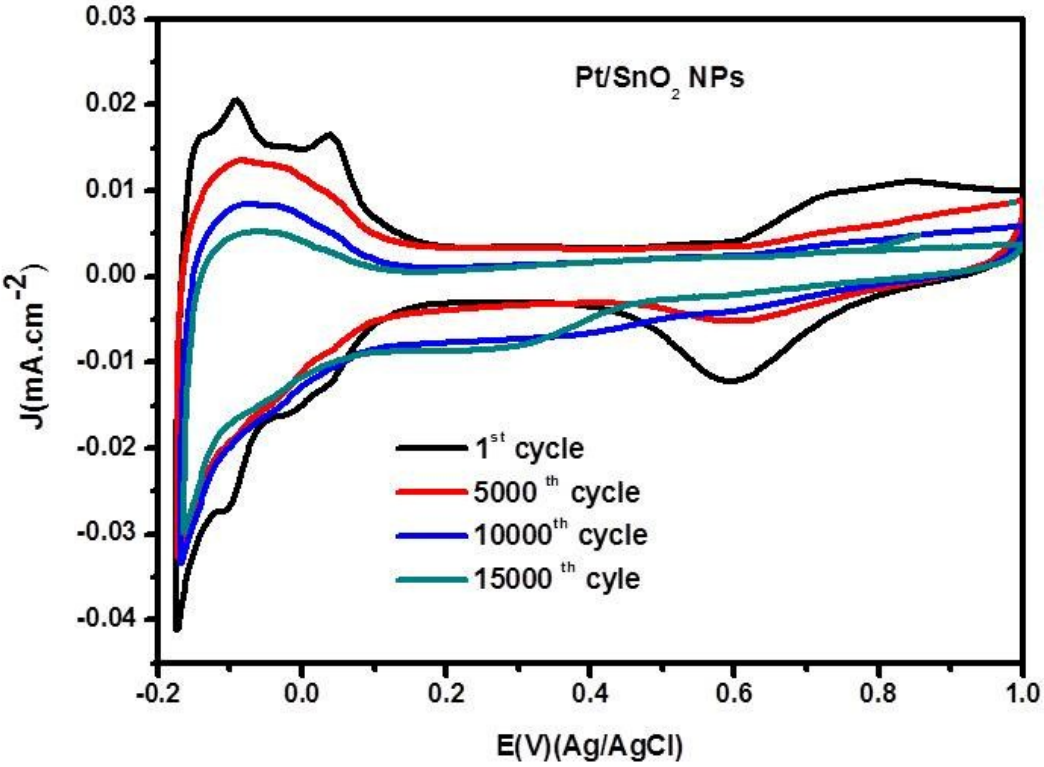

S14. Cyclic voltammograms of the Pt/SnO_2 NPs, recorded in between the stability test conducted in 0.5 M H_2SO_4 between +0.6 and +1.2V at a scan rate of 50 mVs^{-1}. The given curves were measured at a scan rate of 20 mVs^{-1}.

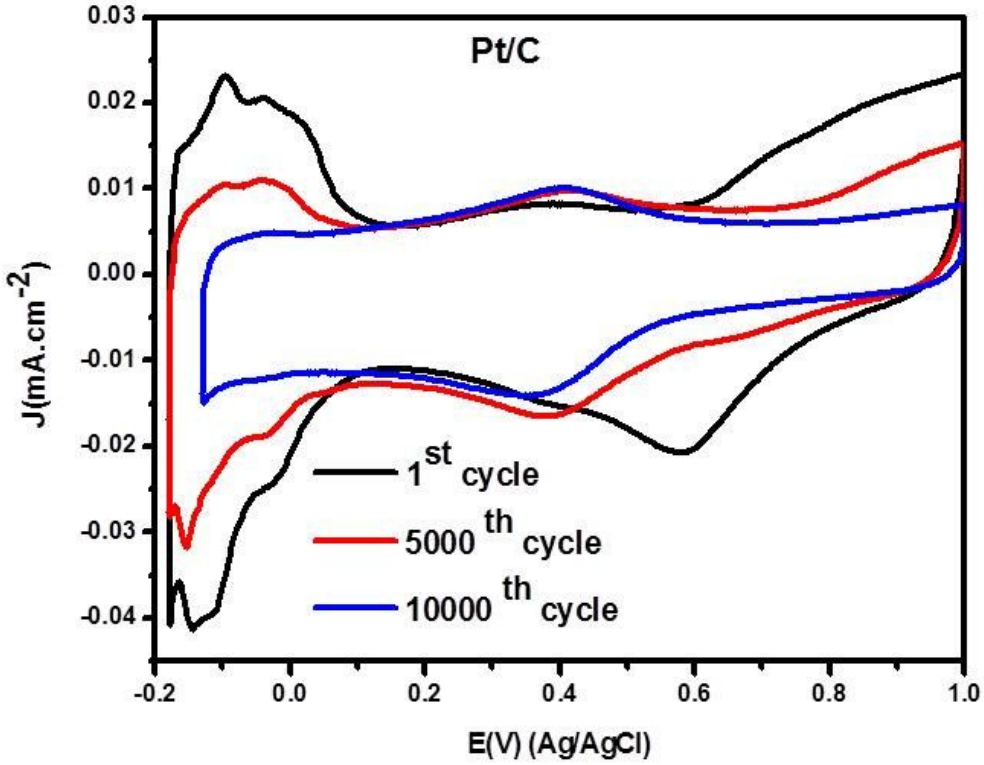

S15. Cyclic voltammograms of the Pt/C, recorded in between the stability test conducted in 0.5 M H_2SO_4 between +0.6 and +1.2V at a scan rate of 50 mVs^{-1}. The given curves were measured at a scan rate of 20 mVs^{-1}.

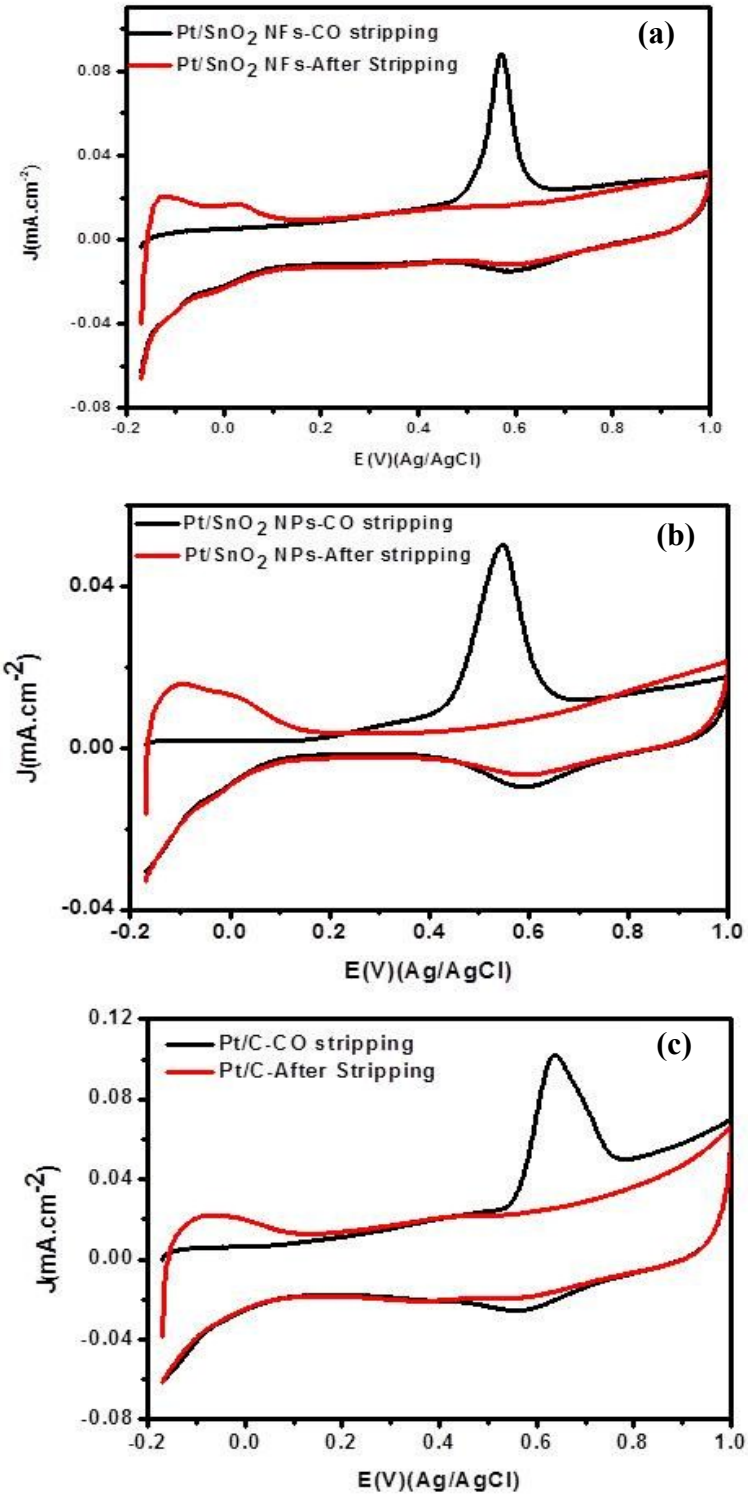

S16. CO-stripping profiles for the (a) Pt/SnO_2 NFs and (b) Pt/SnO_2 NPs and (c) Pt/C, acquired in 0.5 M H_2SO_4 at a scan rate of 20 mVs^{-1}.

3.7. PL spectra

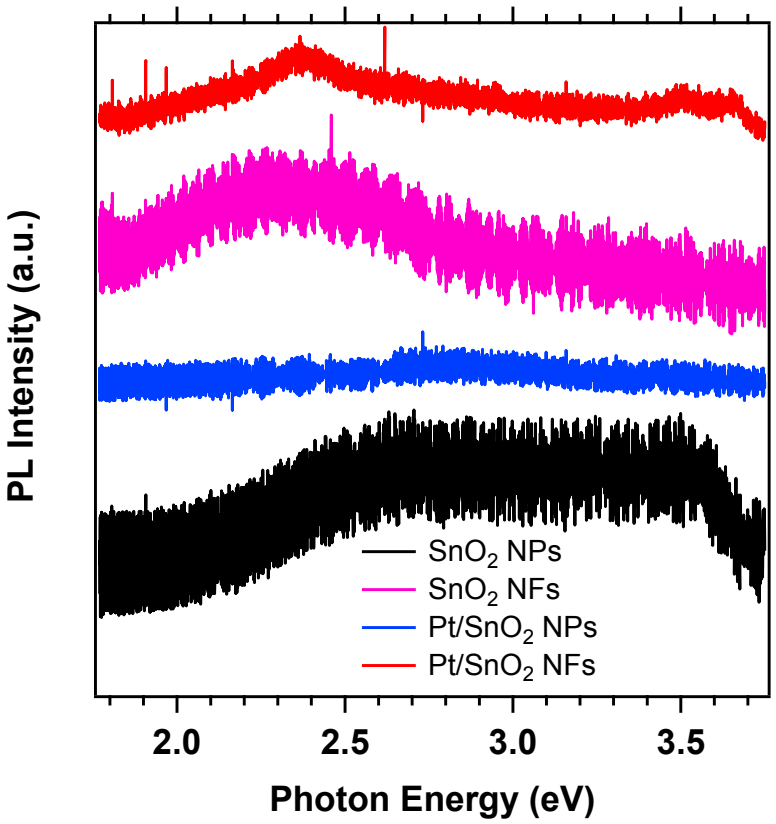

S17. PL emission spectra for the Pt/SnO_2 NFs, SnO_2 NFs, Pt/SnO_2 NFs and Pt/SnO_2 NPs. Measurement temperature: 300 K.

3.8. Energy diagram

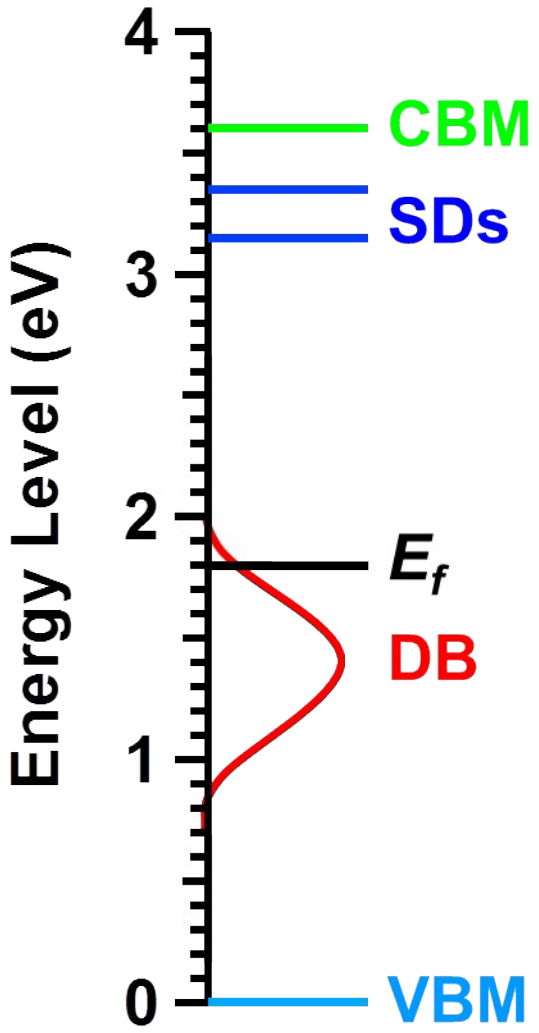

S18. Energy diagram for the SnO_2 NFs, experimentally determined by HAXPES and PL. The abbreviations in the panel, CBM, SDs, E_f, DB and VBM correspond to Conduction-band minimum, Shallow donors, Fermi level, Defect band and Valence-band maximum, respectively.

3.9. AFM/KFM

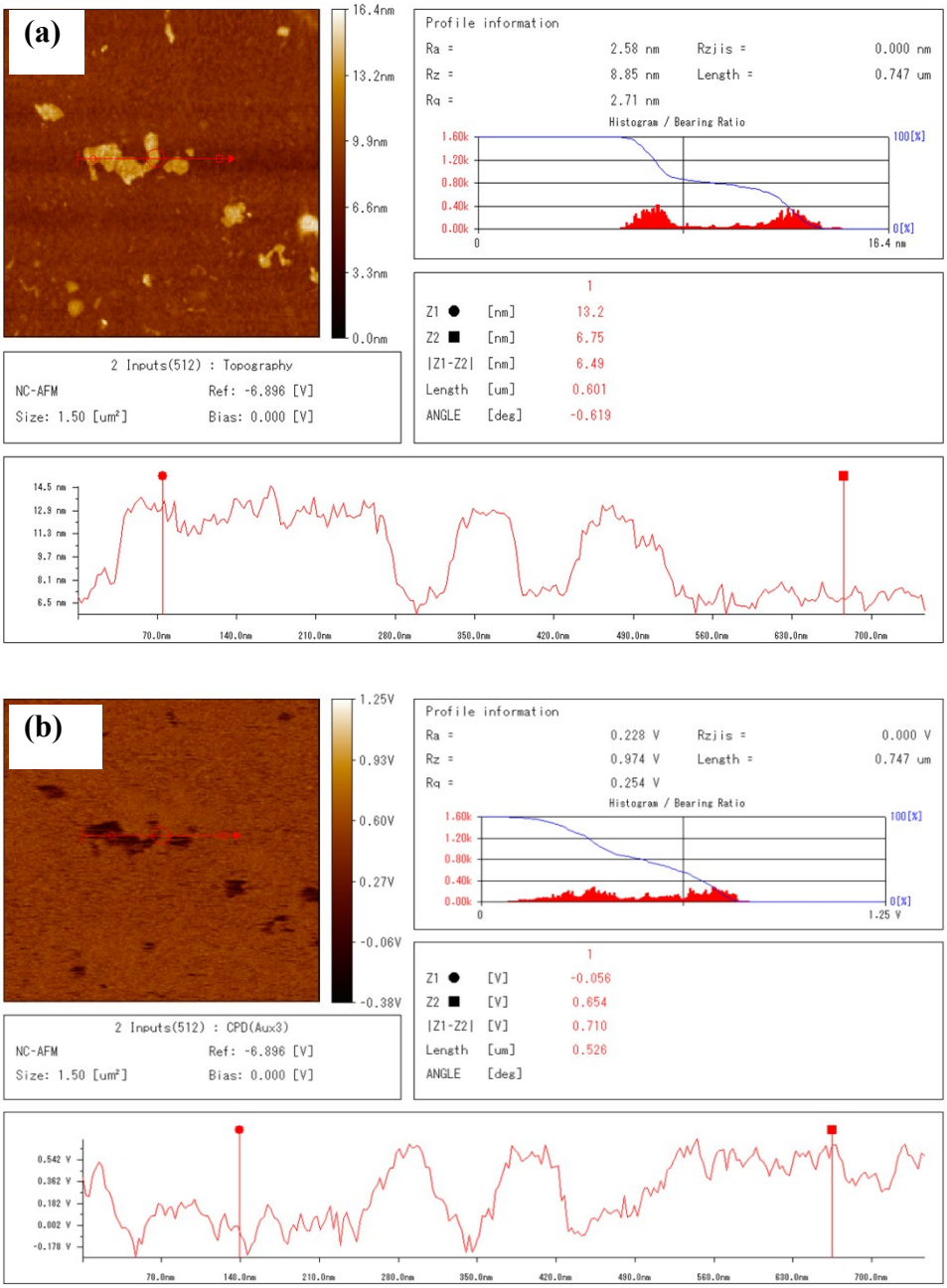

S19. Low-magnification (a) AFM- and (b) KFM images of the Pt/SnO_2 NFs.